Effects of Metal Ions on the Reactivity and Corrosion Electrochemistry of Fe/FeS Nanoparticles

ARTICLE *in* ENVIRONMENTAL SCIENCE & TECHNOLOGY · FEBRUARY 2014

Impact Factor: 5.33 · DOI: 10.1021/es405622d · Source: PubMed

5 AUTHORS, INCLUDING:

Yoon-Seok Chang
Pohang University of Science and Technology
167 PUBLICATIONS **3,363** CITATIONS
SEE PROFILE

Paul Tratnyek
Oregon Health and Science University
151 PUBLICATIONS **6,517** CITATIONS
SEE PROFILE

Environmental Science & Technology

Article

pubs.acs.org/est

Effects of Metal Ions on the Reactivity and Corrosion Electrochemistry of Fe/FeS Nanoparticles

Eun-Ju Kim,[†] Jae-Hwan Kim,[†] Yoon-Seok Chang,*[,†] David Turcio-Ortega,[‡] and Paul G. Tratnyek*[,‡]

[†]School of Environmental Science and Engineering, Pohang University of Science and Technology (POSTECH), Pohang, 790-784, Republic of Korea

[‡]Institute of Environmental Health, Oregon Health & Science University, Portland, Oregon 97239, United States

Supporting Information

ABSTRACT: Nano-zerovalent iron (nZVI) formed under sulfidic conditions results in a biphasic material (Fe/FeS) that reduces trichloroethene (TCE) more rapidly than nZVI associated only with iron oxides (Fe/FeO). Exposing Fe/FeS to dissolved metals (Pd^{2+}, Cu^{2+}, Ni^{2+}, Co^{2+}, and Mn^{2+}) results in their sequestration by coprecipitation as dopants into FeS and FeO and/or by electroless precipitation as zerovalent metals that are hydrogenation catalysts. Using TCE reduction rates to probe the effect of metal amendments on the reactivity of Fe/FeS, it was found that Mn^{2+} and Cu^{2+} decreased TCE reduction rates, while Pd^{2+}, Co^{2+}, and Ni^{2+} increased them. Electrochemical characterization of metal-amended Fe/FeS showed that aging caused passivation by growth of FeO and FeS phases and poisoning of catalytic metal deposits by sulfide. Correlation of rate constants for TCE reduction (k_{obs}) with electrochemical parameters (corrosion potentials and currents, Tafel slopes, and polarization resistance) and descriptors of hydrogen activation by metals (exchange current density for hydrogen reduction and enthalpy of solution into metals) showed the controlling process changed with aging. For fresh Fe/FeS, k_{obs} was best described by the exchange current density for activation of hydrogen, whereas k_{obs} for aged Fe/FeS correlated with electrochemical descriptors of electron transfer.

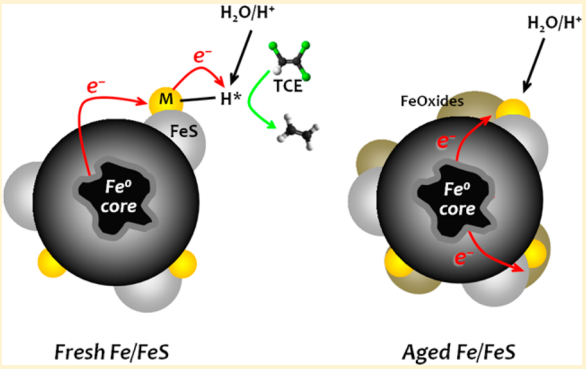

INTRODUCTION

Many approaches to modification of nanoscale zerovalent iron (nZVI) have been investigated for the purposes of providing enhanced performance and/or broader applicability in environmental remediation.[1−6] Much of this work has focused on making nZVI more mobile in porous media by adding various organic polyelectrolytes or surfactants, including carboxymethyl cellulose, polyaspartate, or triblock copolymers (e.g., refs 7−10). Other work has sought to increase the reactivity of nZVI, often by the addition of secondary metals to form bimetallic systems (e.g., Fe/Pd or Fe/Ni), which have been shown to increase contaminant degradation rates and to promote more complete dehalogenation.[11−17] More recently, recognition that nZVI properties are subject to significant "aging" effects has motivated efforts to develop ways of protecting nZVI from nonproductive reactions with the medium (e.g., as composite materials containing organic polymers,[18,19] inorganic carbon,[20−23] silica,[18,24] or clays[25]) or to take advantage of these reactions to extend the long-term performance of nZVI in remediation applications. An example of the latter strategy is the deliberate stimulation of sulfidic conditions in the presence of nZVI, which generates iron sulfides that help preserve the capacity of the system to maintain strongly reducing conditions.[26]

To further explore the benefits of the sulfidation, we have developed a facile method to prepare a multifunctional material composed of nano-zerovalent iron and iron sulfide (Fe/FeS) and have shown that Fe/FeS has advantages over iron oxide coated nZVI (Fe/FeO) with respect to reactivity.[27] However, all of that work was done with simple laboratory model systems (e.g., well-mixed batch reactors prepared with deionized water), so further study under more complex and realistic conditions is needed to evaluate the likely performance of Fe/FeS in remediation applications. As a step toward this goal, we characterized the effects of key environmental variables—including pH, natural organic matter, and the major inorganic cations (Na^+ and Ca^{2+}/Mg^{2+})—on reduction of trichloroethylene (TCE) by Fe/FeS.[28] In the current study, we consider the short- and long-term effects of dissolved transition metal ions, which can interact with Fe^0 in a variety of ways ranging from surface complexation and/or coprecipitation to electroless deposition as zerovalent metals.[29−32] The scenario addressed here is metal exposure after the formation of Fe/FeS (e.g., contaminant metals after remediation with Fe/FeS); the effects

Received: December 17, 2013
Revised: February 25, 2014
Accepted: February 28, 2014
Published: February 28, 2014

   dx.doi.org/10.1021/es405622d | Environ. Sci. Technol. 2014, 48, 4002−4011

of metals included during the formation of Fe/FeS were addressed in a parallel study.[33]

A key determinant of the type of metal interaction with Fe^0 is the reduction potential (E^0) of the metal ions relative to that of Fe^0. The metals investigated here were selected to represent a sufficient range of E^0 values to produce the three classes of interactions described by Li and Zhang[30] (and supported by subsequent work Efecan et al.[34]). As shown in Figure 1, Pd

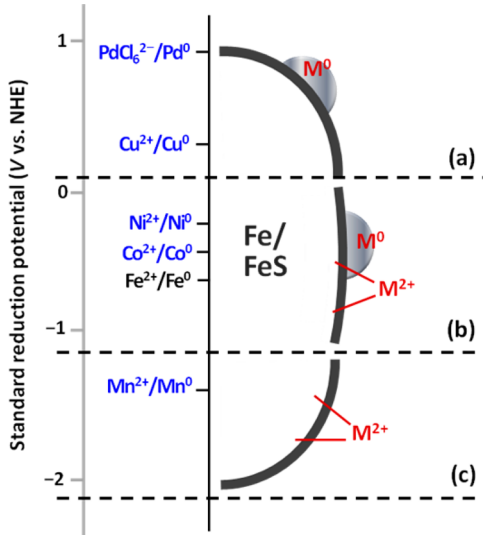

Figure 1. Conceptual model for metal interactions with Fe/FeS. Based on the classification scheme described in Li and Zhang[30] and standard reduction potentials for pH 7 from Pourbaix.[37]

(Pd^{2+} and Pd^{4+}) and Cu^{2+} have substantially more positive E^0 than Fe^0 (Figure 1a), so they should undergo facile reduction to their corresponding zerovalent metals. Ni^{2+} and Co^{2+} have slightly more positive E^0 than Fe^0 (Figure 1b), so they might react by a combination of reduction and complexation (as divalent cations) to the iron oxides (or/and sulfides) on the Fe^0. On the other hand, Mn^{2+} cannot be reduced by Fe^0 because it is more electronegative than Fe^0 (Figure 1c). Instead, Mn^{2+} undergoes sorption onto iron oxides[35] and iron sulfides[36] and may eventually be embedded as a coprecipitate.

The reductive deposition of more electropositive species on Fe^0 results in the iron-based bimetals that, as noted above, generally give greater dechlorination rates than Fe^0 alone. The effect of metals incorporated into the surface oxides or sulfides (e.g., as "dopants") can be faster dechlorination and/or more favorable distributions of reaction products.[14,38−40] However, there appears to be no prior work on the effect of Mn^{2+} on the reduction of chlorinated compounds by treatment with Fe^0, even though modest concentrations (~1 mg/L) are fairly prevalent in groundwater.[41]

The different modes of metal deposition that are represented in Figure 1 imply several possible mechanisms by which the dechlorination rates of organic contaminants might be altered. Where bimetals are formed, their effects are usually interpreted in terms of (*i*) Galvanic coupling between the two metals, (*ii*) hydrogenation catalyzed by the noble metal, (*iii*) conductive islands in the oxide layer, and/or (*iv*) a cathodic shift in corrosion potentials.[13,15,42−47] In this study—on Fe/FeS rather than Fe/FeO—it is also possible that some of the catalytic benefit of bimetals could be poisoned by sulfide.[48−50] For metal ions incorporated into the oxide (or sulfide) film, their effects may be attributed to (*i*) doping of a semiconductor, (*ii*) destabilization of the passive film, or (*iii*) corrosion inhibition by insoluble precipitates.[14,38] It is likely that combinations of the above effects contribute to varying degrees, depending on the metals involved and operational conditions, so systematic characterization of the possible outcomes is challenging. A novel aspect of this study is the use of electrochemical methods to characterize the metal ion effects on nZVI reactivity. For this purpose, electrochemical methods have some unique characteristics (elaborated later) that make them a powerful complement to more common approaches such as microscopy and spectroscopy.

The practical objective of this study was to determine how metal ions—with a representative range of reduction potentials—influence the reactivity of sulfidated nZVI with TCE, so that this information can be used to assess the potential long-term performance of Fe/FeS in field-scale remediation applications. However, the experimental design and scope of this study also provides evidence relevant to several more fundamental questions, including (*i*) how the processes underlying bimetallic effects on nZVI reactivity are influenced by the material changes that arise from aging and (*ii*) how the relative degree of bimetallic enhancement can be described by quantitative property-activity relationships (QPARs). The QPARs developed here may provide a basis for predicting the reactivity of other bimetallic materials, in a manner similar to how quantitative structure−activity relationships (QSARs) are used to predict the reactivity of different contaminant/probe chemicals.

EXPERIMENTAL SECTION

Chemicals and Materials. All of the chemical reagents used were of analytical grade and used as received. Trichloroethene (TCE) was obtained from Sigma-Aldrich (99% purity). Reaction media were prepared by dissolving salts ($FeCl_3{\cdot}6H_2O$, $NaBH_4$, $Na_2S_2O_4$, K_2PdCl_6, $CuCl_2{\cdot}2H_2O$, $NiCl_2{\cdot}6H_2O$, $CoCl_2{\cdot}6H_2O$, $MnCl_2{\cdot}4H_2O$, NaOH, and HCl) in deoxygenated deionized (DO/DI) water. Deoxygenation was performed by sparging with N_2 for 1 h.

The Fe/FeS used in this study was prepared by the reduction of $FeCl_3$ solutions using sodium borohydride in the presence of dithionite, as described previously.[27] In prior work with this material, we have described its structure and composition,[27,28] reactivity with TCE,[27,28] effects of groundwater components,[28] and electrochemical properties.[51] In this study, the metal-amended Fe/FeS was prepared by reacting 2 g/L Fe/FeS with 1 mM solutions of the respective metal salts for 10 min ("fresh") and 15 h ("aged"), respectively. The solution pH for Cu, Co, Ni, and Mn was in the range of 6.5−6.8 and approximately 3.2 for Pd. The solids were recovered by rinsing several times with DO/DI water and drying in a vacuum oven at 50 °C for 1 day.

Characterization. The freeze-dried metal-amended Fe/FeS particles were characterized by high-resolution transmission electron microscopy (HRTEM) and energy-filtered transmission electron microscopy (EFTEM) using a JEM-2200FS microscope with Cs correction. X-ray photoelectron spectra (XPS) were obtained using a VG ESCALAB 220iXL with a monochromatic Mg Kα (1253.6 eV) excitation source.

Batch Experiments and Analysis. The dechlorination of TCE was determined in batch experiments using a protocol very similar to that used in other work on Fe/FeS.[27,28] In brief, 40 mL glass vials were filled with 0.08 g of the Fe/FeS and ~40

dx.doi.org/10.1021/es405622d | Environ. Sci. Technol. 2014, 48, 4002−4011

mL of 0.11 mM TCE in DO/DI water. Vials were capped with Teflon Mininert valves and then placed on a rolling mixer (15 rpm) at room temperature. All experiments were done in triplicate. The aqueous concentrations of TCE and its chlorinated products were measured using a headspace gas chromatograph equipped with an electron capture detector (GC-ECD, HP Agilent 6890), as described previously.[27] Typical products (e.g., ethane and butane) were observed but were not quantified.

Electrochemical Methods. The electrochemical properties of metal amended, fresh and aged Fe/FeS were measured in a three-electrode cell containing a stationary powder disk electrode (PDE) as the working electrode, a Pt wire counter electrode, a Ag/AgCl reference electrode, and 10 mM NaCl as the electrolyte. All potentials are reported vs the Ag/AgCl reference electrode. For each material, duplicate PDEs were prepared by pressing (dry) metal-amended Fe/FeS powders into the electrode cavity in an anaerobic glovebox. Details on the design of the PDE and its use in electrochemical studies of fine-grained metal powders have been reported previously.[52,53]

As in our other recent work with PDEs of Fe/FeS,[51] we performed electrochemical characterization methods in a sequence that proceeds from less-destructive to more-destructive of the working electrode material. First, we performed open-circuit chronopotentiometry (CP), followed by electrochemical impedance spectroscopy (EIS) in the frequency range of 10 kHz to 10 mHz, and finally linear sweep voltammetry (LSV) by polarizing the PDE from −0.25 mV to +1.1 V relative to the open circuit potential at a scan rate of 0.1 mV/s. Electrochemical experiments were performed in a deaerated cell with an Autolab PGSTAT30 (EcoChemie, Utrecht, The Netherlands).

RESULTS AND DISCUSSION

Structure and Composition of Metal-Amended Fe/FeS. Characterization of the structure of metal-amended Fe/FeS using TEM (Figure S1) showed that all of the preparations were composed of irregular, 10−20 nm primary particles similar to those described previously for Fe/FeS without added metals.[27] The high degree of aggregation that is evident in Figure S1 is likely due to sample preparation for microscopy[54] because suspensions of all the materials used in this study were stable for hours.

The EFTEM images of unaged Fe/FeS in Figure S2 show that S-containing material, presumably FeS,[27] is nonuniformly distributed on aggregates that are largely Fe^0 and iron oxides. Most of the amendment metals appear to be concentrated on the Fe/FeO, although some appears to be associated with the FeS. Incorporation of transition metals into FeS and their impact on reductive dechlorination has been described previously.[39,55] The elemental maps for Cu, Mn, Ni, and Pd indicate a nonuniform distribution of these additives, which is consistent with previous observations on bimetallic nanoparticles.[14,15] In contrast, the EFTEM for Co suggests that this element is distributed relatively uniformly throughout the Fe/FeS. The changes in elemental distribution with aging were examined by EFTEM for Fe/FeS/Pd and Fe/FeS/Ni (Figure S3). The most noteworthy change in the distribution of Pd and Ni on the Fe/FeS surface is that Pd is more strongly associated with S than Ni.

In all cases except Mn, the quantity of added metals was the same because they were prepared with equal molar concentrations and all of the metals were deposited (Table S1). For Mn, only about 60% was deposited, presumably because adsorption was the only mechanism.

Characterization of the surface composition of metal-amended Fe/FeS by XPS (Figure S4) showed the metal additives in the oxidation states predicted by the conceptual model in Figure 1. The Cu- and Pd-amended Fe/FeS had amendments only in metallic states; Ni- and Co-amended Fe/FeS were in both metallic and ionic states, whereas Mn was only found in the ionic state on the Fe/FeS surface. These data are not sufficient to determine if the spatial distribution of metal amendments is segregated by valence state (e.g., reduced metals deposited onto Fe^0 and divalent metals adsorbed onto iron oxides/sulfide), but the sequence of steps used to produce these materials is likely to favor their deposition onto the oxide/sulfide phases.

This view of the structure of metal-amended Fe/FeS requires that reduction of the adsorbed metals (in this study: Pd, Cu, Ni, and Co) by Fe^0 should be mediated by its coating of iron oxide and sulfide phases. Possible mechanisms for this were discussed by Li and Zhang[30] using a conceptual model developed for the reduction of organic contaminants by Fe/FeO.[56,57] The latter studies concluded that the most likely process for passing charge through the oxide layer on Fe^0 under environmental remediation conditions is resonance tunneling via localized states (i.e., defects of various types). This process becomes more favorable as the iron oxides become more mixed-valent (and therefore conductive)[58] or replaced by iron sulfides (which generally have smaller band gaps, and therefore are more conductive, than iron oxides[59]). However, the Fermi potential of iron sulfides (roughly 0.4 V at pH 7[59]) is more positive than iron oxides on Fe^0 (typically −0.25 V[57]), which means the iron sulfides provide less driving force for reduction of adsorbates (metals or organics), and this will favor slower kinetics of adsorbate reduction by iron sulfides.

Effect of Metal Ions on TCE Reduction Kinetics. The concentration vs time plots for TCE reduction by fresh and aged metal-amended Fe/FeS are shown in Figure S5, and the rate constants (k_{obs}) obtained by fitting these data to pseudo-first-order kinetics are given in Table S2. The results are summarized in Figure 2, together with data for equivalent experimental conditions that were reported in our previous work on Fe/FeS.[27,28] The comparison shows that the overall increase in k_{obs} due to synthesis in the presence of dithionite is roughly 1 order of magnitude, regardless of the effects of solution chemistry on k_{obs}. In contrast, the metal amendments studied here have relatively large effects on k_{obs}, including enhancements by Co, Ni, and Pd that are about 1 order of magnitude relative to Fe/FeS without metal amendments. The same trends would be apparent if Figure 2 was based on mass- or surface-area-normalized rate constants (because the Fe/FeS mass load and specific surface area are nearly constant across all of these experiments).

The top row in Figure 2 shows that while amendment with Pd, Ni, and Co increased k_{obs}, Cu and Mn caused k_{obs} to decrease (relative to the control without metal amendments) for both fresh and aged Fe/FeS. The inhibitory effect of Cu is opposite the result that has been reported in most previous work using Fe/FeO,[14,15,17,31,60,61] although most of these studies were done with other contaminants (carbon tetrachloride and 1,1,1-trichloroethane) and/or different methods of introducing the metal additives. The effect of Cu observed here is, however, consistent with the electrochemical data discussed below. The inhibitory effect of Mn^{2+} on TCE reduction is most

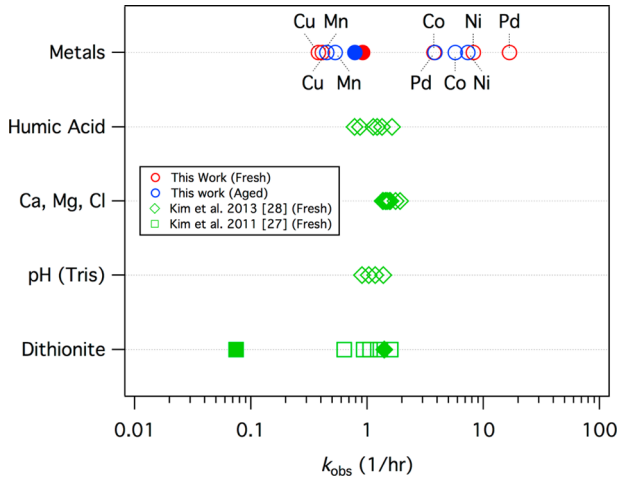

Figure 2. Summary of k_{obs} for TCE reduction by Fe/FeS vs composition of the particles and the medium. (○) Effects of metal amendments (this study). (◊) Effects of solution composition.[28] (□) Effect of dithionite dose during synthesis.[27] Solid symbols are controls: (●) without metal amendments, (◆) in DI water, and (■) without dithionite.

easily interpreted as the result of interspecies competition for surface sites, which has been measured and modeled for a variety of analogous systems (e.g., refs 56, 62−65).

The top row of Figure 2 also shows how aging changes the relative reactivities of Fe/FeS with the various metal amendments: the order of k_{obs} vs metal amendment is the same (Cu < Mn < Co < Ni) except for Pd, which has the highest k_{obs} for fresh Fe/FeS but intermediate k_{obs} for aged Fe/FeS. Another perspective on these data is presented in Figure 3, which shows that rate constants for aged and unaged Fe/FeS plot very close to a 1:1 correlation for all metals except Pd.

The anomalous behavior of Pd-amended Fe/FeS may reflect a greater decrease in catalytic activity of Pd—compared with Co and Ni—due to poisoning by sulfide. Both Ni- and Pd-based hydrogenation catalysts are highly susceptible to poisoning upon exposure to sulfur species,[67,68] and the initial step of sulfur adsorption onto these metals has been studied in great detail.[69,70] Conversely, Pd, Ni, and other "soft" metals have relatively high affinities for iron sulfides (also soft), compared with hard metal ions like Mn^{2+}, and this has been used to rationalize the relative rates of hexachloroethane reduction by metal-amended mackinawite.[39] The data for absolute hardness of the metals shown in Figure 3 reveal that the anomalously low reactivity of aged Pd-amended Fe/FeS is consistent with the substantially lower hardness of Pd compared with Co and Ni. This hypothesis is supported by the stronger association of Pd with S than Ni, as shown in Figure S3. However—or, in addition—the large decrease in reactivity of Fe/FeS/Pd with aging may arise because Pd is a more active hydrogenation catalyst than Ni, and therefore the relative role of atomic hydrogen in the fresh Fe/FeS/Pd system might be larger.[47] Regardless of the cause, if the observed difference between Ni- and Pd-based bimetallic reductants also applies under groundwater remediation conditions, then it might make the enhancement of contaminant reduction by Ni more sustainable than that of Pd. In the long run, however, the accelerated corrosion rate of Fe/FeS amended with Co, Ni, or Pd (based on electrochemical results in the following section) will contribute to detachment and/or occlusion of the catalytic metals, and therefore a gradual decline in their catalytic benefit.[47,71,72]

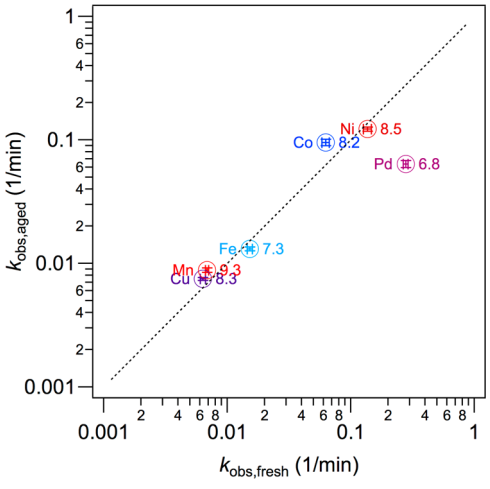

Figure 3. Plot of k_{obs} values for fresh particles vs those for aged particles. Data from Table S1. Dashed line is 1:1. Error bars, based on SD from fitting first-order kinetics, are shown but are smaller than the markers. Absolute hardness (from ref 66) is given as labels.

Effect of Metal Ions on Electrochemical Corrosion Properties. The results presented in the previous section—kinetics of TCE reduction by metal-amended Fe/FeS—constitute a probe reaction approach to characterizing the reactivity of these materials. A distinctly different, but complementary, approach involves electrochemical characterization of powder disk electrodes (PDEs) made by packing the various preparations of metal-amended Fe/FeS using the approach we developed in prior work.[51,52] In one recent study,[51] we used PDEs to characterize the effect of solution conditions on corrosion of Fe/FeS, but that study did not address the effects of aging Fe/FeS, and no prior work has been reported on the electrochemical behavior of bimetallic forms of ZVI. In this study, electrochemical characterization methods were applied to PDEs made from metal-amended Fe/FeS in a sequence from least destructive of the sample to relatively more destructive (chronopotentiometry, then electrochemical impedance spectroscopy, and finally linear sweep voltammetry) in the presence of a common electrolyte, but the following presentation of the results is arranged with the potential-based methods grouped first followed by impedance methods.

The chronopotentiograms (CPs) in Figure S6 show the change in open-circuit potential (E_{oc}) during the first 60 min after immersion of each material into the electrolyte. For unamended Fe/FeS, the values and gradual decline in E_{oc} are consistent with results we have reported previously for this material.[51] For fresh metal-amended Fe/FeS (Figure S6a), most of the metal additives result in very stable values of E_{oc}, which suggests little depassivation of these materials over the time period of this measurement. In contrast, the CPs of aged particles (Figure S6b) show more diverse and dynamic behavior, with consistently less negative E_{oc} values. All of these effects are consistent with the presence of metastable forms of FeO and FeS that developed during aging, which will be relatively labile to transformations upon immersion. In most cases, however, E_{oc} became approximately constant by about 30 min, suggesting that relatively stable experimental conditions existed during the subsequent electrochemical characterizations.

dx.doi.org/10.1021/es405622d | Environ. Sci. Technol. 2014, 48, 4002−4011

Figure S7 shows the linear sweep voltammograms (LSVs) obtained by polarizing each electrode over a range of 1.25 V relative to the E_{oc} (determined from the CP results) at a sufficiently slow scan rate to ensure approximately steady-state conditions. Tafel analysis gave the values of corrosion potential (E_{corr}), corrosion current (i_{corr}), anodic and cathodic Tafel slopes (β_a and β_c), and polarization resistance (R_p) that are given in Table S3. The results for E_{corr} are summarized in Figure 4, together with data for related experimental conditions

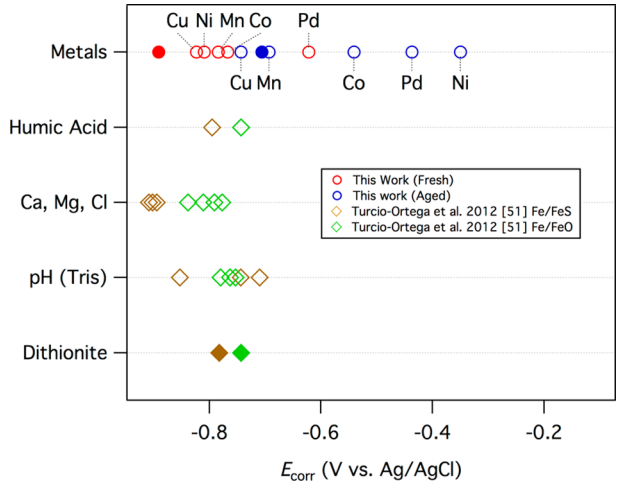

Figure 4. Summary of E_{corr} vs composition of the particles and the medium. (○) Effects of metal amendments (this study). (◊) Effects of solution composition.[51] Solid symbols are controls: (●) without metal amendments and (◆) in DI water. All data from Turcio-Ortega et al.[51] are without aging.

that were reported in our previous work on unamended Fe/FeS.[51] After aging, all of the E_{corr} data shifted toward more positive values, consistent with changes that favor anodic processes ($Fe^0 \rightarrow Fe^{2+}$, FeO, and FeS) over the cathodic process ($H^+ \rightarrow H_2$). In this system, the metal amendments should favor anodic processes by maintaining the conductivity of the FeO and FeS phases formed during aging (according to one or more of the mechanisms discussed in the Introduction). The effect of aging on the cathodic process in this system is likely dominated by gradual poisoning of metal-catalyzed hydrogen reduction by sulfide. In comparison, E_{corr} varies relatively little for fresh Fe/FeS (and Fe/FeO) over all the solutions conditions tested in this and previous work.

The other electrochemical parameters obtained by Tafel analysis (β_c, β_a, R_p, and i_{corr}) are summarized in Figure S8. From the upper-left three panes in Figure S8 (a, b, and e), it appears that β_a is consistently greater than β_c, as was seen in our earlier work without metal amendments,[51] and as expected for porous electrodes made from materials with relatively high resistivity.[73] Comparing data for fresh (red) and aged (blue) Fe/FeS in these three panes reveals that aging generally increased β_c but did not affect β_a. The most straightforward interpretation of this result is that the dominant process during aging of metal-amended Fe/FeS is sulfide poisoning of hydrogen reduction. There appears to be no correlation between the Tafel slopes and R_p or i_{corr} (Figure S8c, d, f, and g), but R_p vs i_{corr} exhibits a strong, inverse, nonlinear relationship (Figure S8i). All of the data in Figure S8i fit well to the expected model ($R_p = B/i_{corr}$) giving an estimate of $B = 53 \pm 2$ mV. (Alternatively, using β_a and β_c from Table S3 and the Stearn-Geary equation[74] gives a range of values of B that average to 52 ± 3.) The consistency of these results across all of the treatments tested suggests that the general robustness of the PDE response extends to the range of materials studied here. However, the estimated values of B are considerably larger than expected under conditions that are well-suited for LPR methods, which should be ~25 mV or less.[74,75] This result is likely due to the relatively high resistance of the solution and particle surface films under the conditions of this study. Similar interpretations were given for the high Tafel slopes obtained in our previous work with PDEs made from Fe/FeO and Fe/FeS[51] and in a recent study with powder microelectrodes made from iron oxides and sulfides.[76] In such cases, electrochemical methods that better accommodate high resistivity, such as EIS, may be more appropriate.

The results obtained by EIS are shown as Bode plots: phase-angle vs frequency (Figure S9) and log |Z| (modulus) vs frequency (Figure S10). The data for unaged, unamended Fe/FeS are qualitatively similar to the EIS reported previously (for 10 mM NaCl),[51] including the relative lack of distinctive features consistent with a high degree of overall passivation for all these materials. As seen in Figure S9, the fresh particles gave larger phase angles at low frequencies and generally more consistent phase-angles over the whole frequency range. Both behaviors were affected by the growth and diversification of passivating materials (FeO and/or FeS) during aging.

In the Bode-modulus plot (Figure S10), the impedance at high frequency reflects the ohmic resistance R_s, and the difference between impedance at low- and high-frequency represents the charge transfer resistance R_{ct}. As seen in Figure S10a, the metal amendments for fresh particles had little effect on R_s (because metal dissolution should be insignificant), whereas R_{ct} exhibited substantial differences, presumably due to one or more of the possible effects of metal amendments discussed in the Introduction (metal doping of the passive film, etc.). In comparison, all of the aged materials (Figure S10b) gave higher and more variable R_s and especially R_{ct}, consistent with accumulation of relatively less conductive, authigenic forms of FeO and FeS. The conditions that lead to high R_{ct}, support less rapid charge-transfer at the Fe/FeS surfaces, which should produce less rapid reduction of contaminants, and conversely, materials with low R_{ct} are expected to produce more rapid contaminant reduction. This hypothesis is tested in the analysis that follows.

Correlation between k_{obs} and Electrochemical Parameters. Correlation analysis on the various quantitative measures of reactivity that we obtained for metal-amended Fe/FeS is a potentially powerful approach to evaluate the mechanism of metal effects in this system, and a strong correlation involving contaminant degradation rates (in this case, k_{obs} for TCE reduction) could even lead to quantitative property−activity relationships (QPARs) for predicting the effect of other metals and, thereby, providing direction for future work.

Scatter plots showing the correlation between rate constants for TCE reduction (k_{obs}; from Table S2) and three electrochemical variables (E_{corr}, i_{corr}, and R_p; from Table S3) are given in Figure 5. The data for fresh Fe/FeS with the various metal amendments gave poor correlations (Figure 5a−c), but the aged materials show promising correlations to all three electrochemical parameters (Figure 5d−f). Since i_{corr} is a nearly direct measure of the Fe/FeS corrosion rate, the positive correlation between k_{obs} and i_{corr} (Figure 5e) suggests that the rate of TCE reduction was closely related to the corrosion rate for these materials. This relationship and that between i_{corr} and

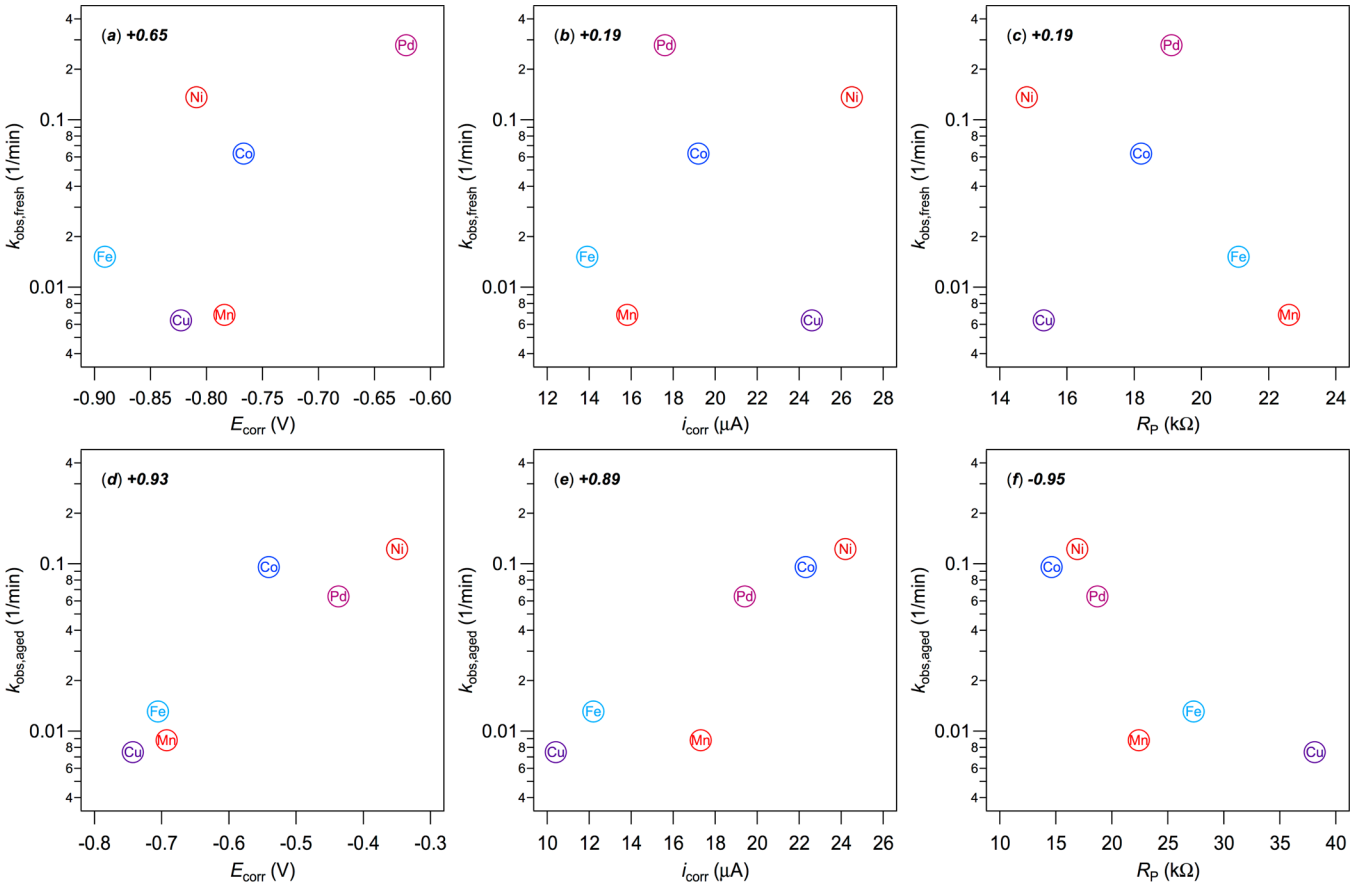

Figure 5. Correlations between electrochemical corrosion parameters and log k_{obs} for (top row) fresh Fe/FeS and (bottom row) aged Fe/FeS. Correlation coefficients are given in italics. Rate constants from Table S2 and descriptor data from Table S3.

R_p (recall the above discussion of Figure S8i) results in the good negative correlation between k_{obs} and R_p shown in Figure 5f. The strong positive correlation between k_{obs} and E_{corr} (Figure 5d) would be surprising if the controlling factors were the same as those responsible for the negative correlation we saw in an earlier study on carbon tetrachloride reduction by aging nZVI.[77] However, in preliminary, unpublished work on carbon tetrachloride and nitrobenzene reduction by aged nZVI in the presence of natural organic matter (NOM), we found positive correlations analogous to that shown in Figure 5d. This pattern could arise if, for example, the less strongly reducing material deposited during aging (FeO/FeS or NOM) becomes the dominant phase on which contaminant reduction takes place. To fully test this hypothesis may require control experiments with simpler model systems and column or larger-scale tests to simulate changes in the overall balance of factors under field conditions.

While Figure 5 shows fairly strong correlations between k_{obs} and three electrochemical properties of the aged particles, the lack of a correlation in the fresh particles suggests that nonelectrochemical processes are controlling. Among the other mechanisms that may contribute to the rate enhancements by bimetallic reductants, the major nonelectrochemical alternative is the hypothesis that the metal additive would catalyze the formation of reactive hydrogen species (adsorbed or dissolved atomic hydrogen or hydride), which then might contribute to contaminant reduction by hydrogenation. Therefore, to test the possible involvement of hydrogen in these systems, we examined the correlation of k_{obs} to the several potentially relevant descriptors of the amending metals. One such descriptor is the partial molar enthalpy for an infinitely dilute solution of hydrogen in pure metals (ΔH_H^∞),[78] which was effective for describing the enhanced reduction of 1,1,1-trichloroethane (TCA) by bimetallic reductants.[15] Another logical descriptor is the exchange current density (i_0) for hydrogen evolution on pure metal electrodes,[79] which has been considered in prior work[15,17] but did not give significant correlations to k_{obs} for the reduction of TCA or TCE by ZVI with various catalytic bimetals. Additional descriptors were considered in this study—such as the solubility of hydrogen in pure metals[80]—but they did not produce correlations with distinctive benefits, so they are not discussed below.

As shown in Figure 6, ΔH_H^∞ did not produce a meaningful correlation with k_{obs} for either fresh or aged Fe/FeS, but i_0 gave promising correlations, especially with the data for the fresh materials (Figure 6b). Since i_0 is a relatively direct measure of the expected rates of hydrogen evolution on various metals, the correlation between this descriptor and k_{obs} suggests a close link between formation of active hydrogen species and the reduction of TCE in this system. Experimental measurement of hydrogen evolution—as was done by Lin et al.[17]—might have produced comparable results, but such an approach does not have the generality provided by a descriptor such as i_0, for which standard values are well established.[79,81] The correlation between k_{obs} and i_0 is strong for fresh, amended Fe/FeS but weaker for the aged materials (Figure 6b vs d), as might be expected if accumulation of authigenic FeO and FeS during aging limits direct access to the metals that favor activation of

dx.doi.org/10.1021/es405622d | Environ. Sci. Technol. 2014, 48, 4002−4011

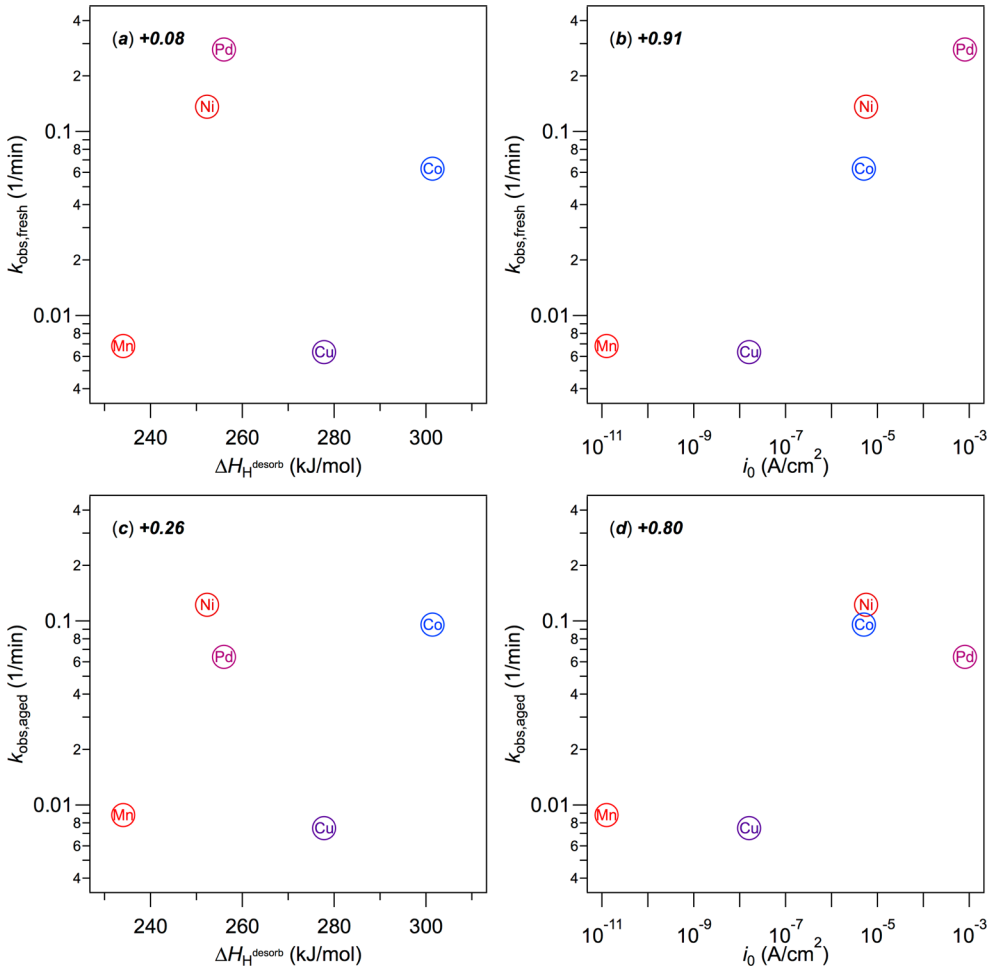

Figure 6. Correlations between hydrogenation-related parameters and log k_{obs} for (top row) fresh Fe/FeS and (bottom row) aged Fe/FeS. Correlation coefficients are given in italics. Rate constants from Table S1 and descriptor data from Table S3.

hydrogen. This process might cause a shift toward conditions where the overall processes controlling contaminant reduction rates involve electron transfer without mediation by hydrogen, and that would be consistent with the correlations between k_{obs} and electrochemical descriptors for the aged Fe/FeS (Figure 5d–f).

Implications. Taken together, the results of this study illustrate the challenge of assessing the overall benefit of specific enhancements to remediation processes that ultimately are to be applied in complex and dynamic environmental systems. In this case, the high rate of TCE reduction obtained from nZVI produced under sulfidic conditions (Fe/FeS) was even greater when Fe/FeS was amended with metals that undergo electroless reduction to hydrogenation catalysts (Co, Ni, and Pd). For comparatively fresh metal-amended Fe/FeS, the enhancement appears to be due to the formation of active forms of hydrogen. However, allowing the material to age results in accumulation of additional FeO/FeS and partial poisoning of the phases that catalyze hydrogenation. Therefore, in real environmental engineering applications, it is not clear that the benefits observed in this study will be sufficiently long-term to be significant. Even if a net benefit is sustained over the long-term, the results of this study suggest that the mechanism of the enhancement may change (from hydrogenation on catalytic metals to electron transfer on reduced iron oxides and sulfides). This would result in changes in the relative reactivity of different contaminants, degradation pathways taken, and products formed from each (as evidenced by recent results with kinetic isotope effects[47]). With respect to the removal of metals, as cocontaminants with chlorinated solvents, this study shows that the former may be beneficial to the latter, even over a wide range of metals and degrees of aging in the presence of sulfide.

■ ASSOCIATED CONTENT

Supporting Information

Primary data are presented from material characterization methods (TEM, EFTEM, XPS), reactivity (TCE reduction kinetics), electrochemistry (CP, EIS, and LSV, and tables of electrochemical parameters obtained by Tafel analysis), and correlation analysis (electrochemical and hydrogenation descriptors). This material is available free of charge via the Internet at http://pubs.acs.org.

■ AUTHOR INFORMATION

Corresponding Authors

*Phone: +82-54-279-2281. Fax: +82-54-279-8299. E-mail: yschang@postech.ac.kr..

*Phone: 503-346-3431. Fax: 503-346-3427. E-mail: tratnyek@ohsu.edu.

Notes

The authors declare no competing financial interest.

■ ACKNOWLEDGMENTS

Primary support for this work was from the National Research Foundation of Korea (Grant No. 2011-0028723) and "The GAIA Project" by Korea Ministry of Environment. Resources for the electrochemical aspects of this work came from projects funded by the U.S. Department of Energy, Office of Biological and Environmental Research (ER64222-1027803-0012001) and U.S. National Science Foundation, Environmental Engineering Program (CBET-1333476).

■ REFERENCES

(1) Geiger, C. L.; Carvalho-Knighton, K.; Novaes-Card, S.; Maloney, P.; DeVor, R. A review of environmental applications of nanoscale and microscale reactive metal particles. In *Environmental Applications of Nanoscale and Microscale Reactive Metal Particles*; Geiger, C. L., Carvalho-Knighton, K. M., Eds.; American Chemical Society: Washington, DC, 2009; ACS Symposium Series, Vol. *1027*, pp 1−20.

(2) Crane, R. A.; Scott, T. B. Nanoscale zero-valent iron: Future prospects for an emerging water treatment technology. *J. Hazard. Mater.* **2012**, *211*−*212*, 112−125.

(3) Kharisov, B. I.; Rasika, D. H. V.; Kharissova, O. V.; Manuel, J.-P. V.; Olvera, P. B.; Munoz, F. B. Iron-containing nanomaterials: synthesis, properties, and environmental applications. *RSC Adv.* **2012**, *2*, 9325−9358.

(4) O'Carroll, D.; Sleep, B.; Krol, M.; Boparai, H.; Kocur, C. Nanoscale zero valent iron and bimetallic particles for contaminated site remediation. *Adv. Water Resour.* **2013**, *51*, 104−122.

(5) Tratnyek, P. G.; Salter-Blanc, A. J.; Nurmi, J. T.; Amonette, J. E.; Liu, J.; Wang, C.; Dohnalkova, A.; Baer, D. R. Reactivity of zerovalent metals in aquatic media: Effects of organic surface coatings. In *Aquatic Redox Chemistry*; Tratnyek, P. G., Grundl, T. J., Haderlein, S. B., Eds.; American Chemical Society: Washington, DC, 2011; ACS Symposium Series, Vol. *1071*, pp 381−406.

(6) Yan, W.; Lien, H. L.; Koel, B. E.; Zhang, W.-X. Iron nanoparticles for environmental clean-up: Recent developments and future outlook. *Environ. Sci.: Processes Impacts* **2013**, *15*, 63−77.

(7) He, F.; Zhao, D. Manipulating the size and dispersibility of zerovalent iron nanoparticles by use of carboxymethyl cellulose stabilizers. *Environ. Sci. Technol.* **2007**, *41*, 6216−6221.

(8) Johnson, R. L.; O'Brien Johnson, R.; Nurmi, J. T.; Tratnyek, P. G. Natural organic matter enhanced mobility of nano zero-valent iron. *Environ. Sci. Technol.* **2009**, *43*, 5455−5460.

(9) Saleh, N.; Phenrat, T.; Sirk, K.; Dufour, B.; Ok, J.; Sarbu, T.; Matyjaszewski, K.; Tilton, R. D.; Lowry, G. V. Adsorbed triblock copolymers deliver reactive iron nanoparticles to the oil/water interface. *Nano Lett.* **2005**, *5*, 2489−2494.

(10) Tiraferri, A.; Sethi, R. Enhanced transport of zerovalent iron nanoparticles in saturated porous media by guar gum. *J. Nanoparticle Res.* **2009**, *11*, 635−645.

(11) Barnes, R. J.; Riba, O.; Gardner, M. N.; Scott, T. B.; Jackman, S. A.; Thompson, I. P. Optimization of nano-scale nickel/iron particles for the reduction of high concentration chlorinated aliphatic hydrocarbon solutions. *Chemosphere* **2010**, *79*, 448−454.

(12) Cho, Y.; Choi, S.-I. Degradation of PCE, TCE and 1,1,1-TCA by nanosized FePd bimetallic particles under various experimental conditions. *Chemosphere* **2010**, *81*, 940−945.

(13) Tee, Y.-H.; Bachas, L.; Bhattacharyya, D. Degradation of trichloroethylene and dichlorobiphenyls by iron-based bimetallic nanoparticles. *J. Phys. Chem. C* **2009**, *113*, 9454−9464.

(14) Chun, C. L.; Baer, D. R.; Matson, D. W.; Amonette, J. E.; Penn, R. L. Characterization and reactivity of iron nanoparticles prepared with added Cu, Pd, and Ni. *Environ. Sci. Technol.* **2010**, *44*, 5079−5085.

(15) Cwiertny, D. M.; Bransfield, S. J.; Livi, K. J. T.; Fairbrother, D. H.; Roberts, A. L. Exploring the influence of granular iron additives on 1,1,1-trichloroethane reduction. *Environ. Sci. Technol.* **2006**, *40*, 6837−6843.

(16) Kim, Y. H.; Carraway, E. R. Reductive dechlorination of TCE by zero valent bimetals. *Environ. Technol.* **2003**, *24*, 69−75.

(17) Lin, C. J.; Lo, S.-L.; Liou, Y. H. Dechlorination of trichloroethylene in aqueous solution by noble metal-modified iron. *J. Hazard. Mater.* **2004**, *116*, 219−228.

(18) Meeks, N. D.; Smuleac, V.; Stevens, C.; Bhattacharyya, D. Iron-based nanoparticles for toxic organic degradation: Silica platform and green synthesis. *Ind. Eng. Chem. Res.* **2012**, *51*, 9581−9590.

(19) Smuleac, V.; Varma, R.; Sikdar, S.; Bhattacharyya, D. Green synthesis of Fe and Fe/Pd bimetallic nanoparticles in membranes for reductive degradation of chlorinated organics. *J. Membr. Sci.* **2011**, *379*, 131−137.

(20) Zhan, J.; Sunkara, B.; Tang, J.; Wang, Y.; He, J.; McPherson, G. L.; John, V. T. Carbothermal synthesis of aerosol-based adsorptive-reactive iron-carbon particles for the remediation of chlorinated hydrocarbons. *Ind. Eng. Chem. Res.* **2011**, *50*, 13021−13029.

(21) Tseng, H.-H.; Su, J.-G.; Liang, C. Synthesis of granular activated carbon/zero valent iron composites for simultaneous adsorption/dechlorination of trichloroethylene. *J. Hazard. Mater.* **2011**, *192*, 500−506.

(22) Zhuang, Y.; Ahn, S.; Seyfferth, A. L.; Masue-Slowey, Y.; Fendorf, S.; Luthy, R. G. Dehalogenation of polybrominated diphenyl ethers and polychlorinated biphenyl by bimetallic, impregnated, and nanoscale zerovalent iron. *Environ. Sci. Technol.* **2011**, *45*, 4896−4903.

(23) Choi, H.; Al-Abed, S. R.; Agarwal, S.; Dionysiou, D. D. Synthesis of reactive nano-Fe/Pd bimetallic system-impregnated activated carbon for the simultaneous adsorption and dechlorination of PCBs. *Chem. Mater.* **2008**, *20*, 3649−3655.

(24) Zheng, T.; Zhan, J.; He, J.; Sunkara, B.; Lu, Y.; McPherson Gary, L.; Piringer, G.; Kolesnichenko, V.; John, V. T. Nanostructured multifunctional materials for environmental remediation of chlorinated hydrocarbons. In *Environmental Applications of Nanoscale and Microscale Reactive Metal Particles*; Geiger, C. L., Carvalho-Knighton, K. M., Eds.; American Chemical Society: Washington, DC, 2009; ACS Symposium Series, Vol. *1027*, pp 163−179.

(25) Kadu, B. S.; Chikate, R. C. NZVI based nanocomposites: Role of noble metal and clay support on chemisorptive removal of Cr(VI). *J. Environ. Chem. Eng.* **2013**, *1*, 320−327.

(26) Fan, D.; Anitori, R. P.; Tebo, B. M.; Tratnyek, P. G.; Lezama Pacheco, J. S.; Kukkadapu, R. K.; Engelhard, M. H.; Bowden, M. E.; Kovarik, L.; Arey, B. W. Reductive sequestration of pertechnetate ($^{99}TcO_4^-$) by nano zero-valent iron (nZVI) transformed by abiotic sulfide. *Environ. Sci. Technol.* **2013**, *47*, 5302−5310.

(27) Kim, E.-J.; Kim, J.-H.; Azad, A.-M.; Chang, Y.-S. Facile synthesis and characterization of Fe/FeS nanoparticles for environmental applications. *ACS Appl. Mater. Interfac.* **2011**, *3*, 1457−1462.

(28) Kim, E.-J.; Murugesan, K.; Kim, J.-H.; Tratnyek, P. G.; Chang, Y.-S. Remediation of trichloroethylene by FeS-coated iron nanoparticles in simulated and real groundwater: Effects of water chemistry. *Ind. Eng. Chem. Res.* **2013**, *52*, 9343−9350.

(29) Khudenko, B. M.; Gould, J. P. Specifics of cementation processes for metals removal. *Water Sci. Technol.* **1991**, *24*, 235−246.

(30) Li, X.-Q.; Zhang, W.-X. Sequestration of metal cations with zerovalent iron nanoparticles - A study with high resolution x-ray photoelectron spectroscopy (HR-XPS). *J. Phys. Chem. C* **2007**, *111*, 6939−6946.

(31) Zhang, W.-X.; Wang, C.-B.; Lien, H.-L. Treatment of chlorinated organic contaminants with nanoscale bimetallic particles. *Catal. Today* **1998**, *40*, 387−395.

(32) Li, X.-Q.; Zhang, W.-X. Iron nanoparticles: The core−shell structure and unique properties for Ni(II) sequestration. *Langmuir* **2006**, *22*, 4638−4642.

(33) Kim, E. J.; Le Thanh, T.; Kim, J. H.; Chang, Y. S. Synthesis of metal sulfide-coated iron nanoparticles with enhanced surface reactivity and biocompatibility. *RSC Adv.* **2013**, *3*, 5338−5340.

(34) Efecan, N.; Shahwan, T.; Eroğlu, A. E.; Lieberwirth, I. Characterization of the uptake of aqueous Ni^{2+} ions on nanoparticles of zero-valent iron (nZVI). *Desalination* **2009**, *249*, 1048−1054.

(35) Coughlin, B. R.; Stone, A. T. Nonreversible adsorption of divalent metal ions (Mn^{II}, Co^{II}, Ni^{II}, Cu^{II}, and Pb^{II}) onto goethite: Effects of acidification, Fe^{II} addition, and picolinic acid addition. *Environ. Sci. Technol.* **1995**, *29*, 2445−2455.
(36) Arakaki, T.; Morse, J. W. Coprecipitation and adsorption of Mn(II) with mackinawite (FeS) under conditions similar to those found in anoxic sediments. *Geochim. Cosmochim. Acta* **1993**, *57*, 9−14.
(37) Pourbaix, M. *Atlas of Electrochemical Equilibria in Aqueous Solutions*; National Association of Corrosion Engineers: Houston, TX, 1974.
(38) Baer, D. R.; Tratnyek, P. G.; Amonette, J. E.; Chun, C. L.; Nachimuthu, P.; Nurmi, J. T.; Penn, R. L.; Matson, D. W.; Linehan, J. C.; Qiang, Y.; Sharma, A., Tuning the properties of iron nanoparticles: Doping effects on reactivity and aging. In *International Environmental Nanotechnology Conference: Applications and Implications (7−9 October 2008)*, Chicago, IL; U.S. Environmental Protection Agency: Washington, DC, 2009; Vol. EPA 905-R09-032, pp 73−78.
(39) Jeong, H. Y.; Hayes, K. F. Impact of transition metals on reductive dechlorination rate of hexachloroethane by mackinawite. *Environ. Sci. Technol.* **2003**, *37*, 4650−4655.
(40) Choi, J.; Choi, K.; Lee, W. Effects of transition metal and sulfide on the reductive dechlorination of carbon tetrachloride and 1,1,1-trichloroethane by FeS. *J. Hazard. Mater.* **2009**, *162*, 1151−1158.
(41) Matthess, G. *The Properties of Groundwater*; Wiley: New York, 1982.
(42) Cheng, I. F.; Fernando, Q.; Korte, N. Electrochemical dechlorination of 4-chlorophenol to phenol. *Environ. Sci. Technol.* **1997**, *31*, 1074−1078.
(43) Kim, J.-H.; Tratnyek, P. G.; Chang, Y.-S. Rapid dechlorination of polychlorinated dibenzo-p-dioxins (PCDDs) by bimetallic and nano-sized zerovalent iron. *Environ. Sci. Technol.* **2008**, *42*, 4106−4112.
(44) Scherer, M. M.; Westall, J. C.; Ziomek-Moroz, M.; Tratnyek, P. G. Kinetics of carbon tetrachloride reduction at an oxide-free iron electrode. *Environ. Sci. Technol.* **1997**, *31*, 2385−2391.
(45) Scherer, M. M.; Westall, J. C.; Tratnyek, P. G. Discussion on "Electrochemical and Raman spectroscopic studies of the influence of chlorinated solvents on the corrosion behaviour of iron in borate buffer and in simulated groundwater" [Corrosion Science 42 (2000) 1921−1939]. *Corros. Sci.* **2001**, *44*, 1151−1157.
(46) Xu, Y.; Zhang, W.-X. Subcolloidal Fe/Ag particles for reductive dehalogenation of chlorinated benzenes. *Ind. Eng. Chem. Res.* **2000**, *39*, 2238−2244.
(47) Xie, Y.; Cwiertny, D. M. Chlorinated solvent transformation by palladized zerovalent iron: Mechanistic insights from reductant loading studies and solvent kinetic isotope effects. *Environ. Sci. Technol.* **2013**, *47*, 7940−7948.
(48) Lim, T.-T.; Zhu, B.-W. Effects of anions on the kinetics and reactivity of nanoscale Pd/Fe in trichlorobenzene dechlorination. *Chemosphere* **2008**, *73*, 1471−1477.
(49) Lin, C. J.; Liou, Y. H.; Lo, S.-L. Supported Pd/Sn bimetallic nanoparticles for reductive dechlorination of aqueous trichloroethylene. *Chemosphere* **2009**, *74*, 314−319.
(50) Agarwal, S.; Al-Abed, S. R.; Dionysiou, D. D. A feasibility study on Pd/Mg application in historically contaminated sediments and PCB spiked substrates. *J. Hazard. Mater.* **2009**, *172*, 1156−1162.
(51) Turcio-Ortega, D.; Fan, D.; Tratnyek, P. G.; Kim, E.-J.; Chang, Y.-S. Reactivity of Fe/FeS nanoparticles: Electrolyte composition effects on corrosion electrochemistry. *Environ. Sci. Technol.* **2012**, *46*, 12484−12492.
(52) Nurmi, J. T.; Bandstra, J. Z.; Tratnyek, P. G. Packed powder electrodes for characterizing the reactivity of granular iron in borate solutions. *J. Electrochem. Soc.* **2004**, *151*, B347−B353.
(53) Nurmi, J. T.; Tratnyek, P. G. Electrochemical studies of packed iron powder electrodes: Effects of common constituents of natural waters on corrosion potential. *Corros. Sci.* **2008**, *50*, 144−154.
(54) Burleson, D. J.; Driessen, M. D.; Penn, R. L. On the characterization of environmental nanoparticles. *J. Environ. Sci. Health, Part A* **2004**, *A39*, 2707−2753.
(55) Jeong, H. Y.; Hayes, K. F. Reductive dechlorination of tetrachloroethylene and trichloroethylene by mackinawite (FeS) in the presence of metals: Reaction rates. *Environ. Sci. Technol.* **2007**, *41*, 6390−6396.
(56) Scherer, M. M.; Balko, B. A.; Tratnyek, P. G. The role of oxides in reduction reactions at the metal-water interface. In *Mineral-Water Interfacial Reactions: Kinetics and Mechanisms*; Sparks, D. L., Grundl, T. J., Eds.; American Chemical Society: Washington, DC, 1998; ACS Symposium Series, Vol. *715*, pp 301−322.
(57) Balko, B. A.; Tratnyek, P. G. Photoeffects on the reduction of carbon tetrachloride by zero-valent iron. *J. Phys. Chem. B* **1998**, *102*, 1459−1465.
(58) Gorski, C. A.; Scherer, M. M. Fe^{2+} Sorption at the Fe oxide-water interface: A revised conceptual framework. In *Aquatic Redox Chemistry*; Tratnyek, P. G., Grundl, T. J., Haderlein, S. B., Eds.; American Chemical Society: Washington, DC, 2011; ACS Symposium Series, Vol. *1071*, pp 315−343.
(59) Xu, Y.; Schoonen, M. A. A. The absolute energy positions of conduction and valence bands of selected semiconducting minerals. *Am. Mineral.* **2000**, *85*, 543−556.
(60) Bransfield, S. J.; Cwiertny, D. M.; Roberts, A. L.; Fairbrother, D. H. Influence of copper loading and surface coverage on the reactivity of granular iron toward 1,1,1-trichloroethane. *Environ. Sci. Technol.* **2006**, *40*, 1485−1490.
(61) Lien, H. L.; Jhuo, Y. S.; Chen, L. H. Effect of heavy metals on dechlorination of carbon tetrachloride by iron nanoparticles. *Environ. Eng. Sci.* **2007**, *24*, 21−30.
(62) Johnson, T. L.; Fish, W.; Gorby, Y. A.; Tratnyek, P. G. Degradation of carbon tetrachloride by iron metal: Complexation effects on the oxide surface. *J. Contam. Hydrol.* **1998**, *29*, 377−396.
(63) Cho, H.-H.; Park, J.-W. Effect of coexisting compounds on the sorption and reduction of trichloroethylene with iron. *Environ. Toxicol. Chem.* **2005**, *24*, 11−16.
(64) Dries, J.; Bastiaens, L.; Springael, D.; Agathos, S. N.; Diels, L. Competition for sorption and degradation of chlorinate ethenes in batch zero-valent iron sytems. *Environ. Sci. Technol.* **2004**, *38*, 2879−2884.
(65) Schäfer, D.; Köber, R.; Dahmke, A. Competing TCE and cis-DCE degradation kinetics by zero-valent iron - experimental results and numerical simulation. *J. Contam. Hydrol.* **2003**, *65*, 183−202.
(66) Parr, R. G.; Pearson, R. G. Absolute hardness: Companion parameter to absolute electronegativity. *J. Am. Chem. Soc.* **1983**, *105*, 7512−7516.
(67) Barbier, I.; Lamy-Pitara, E.; Marecot, P.; Boitiaux, J. P.; Cosyns, J.; Verna, F. Role of sulfur in catalytic hydrogenation reactions. *Adv. Catal.* **1990**, *37*, 279.
(68) Bartholomew, C. H.; Agrawal, P. K.; Katzer, J. R. Sulfur poisoning in metals. *Adv. Catal.* **1982**, *31*, 135−242.
(69) Oudar, J. Sulfur adsorption and poisoning of metallic catalysts. *Catal. Rev.: Sci. Eng.* **1980**, *22*, 171−195.
(70) Rodriguez, J. A.; Chaturvedi, S.; Kuhn, M.; Hrbek, J. Reaction of H_2S and S_2 with metal/oxide surfaces: Band-gap size and chemical reactivity. *J. Phys. Chem. B* **1998**, *102*, 5511−5519.
(71) Yan, W.; Herzing, A. A.; Li, X.-Q.; Kiely, C. J.; Zhang, W.-X. Structural evolution of Pd-doped nanoscale zero-valent iron (nZVI) in aqueous media and implications for particle aging and reactivity. *Environ. Sci. Technol.* **2010**, *44*, 4288−4294.
(72) Zhu, B.-W.; Lim, T.-T. Catalytic reduction of chlorobenzenes with Pd/Fe nanoparticles: Reactive sites, catalyst stability, particle aging, and regeneration. *Environ. Sci. Technol.* **2007**, *41*, 7523−7529.
(73) Doménech-Carbó, A. *Electrochemistry of Porous Materials*; CRC Press: Boca Raton, FL, 2010.
(74) Frankel, G. S. Electrochemical techniques in corrosion: status, limitations, and needs. *J. ASTM Int.* **2008**, *5*, No. JAI101241.
(75) Jones, D. A. *Principles and Prevention of Corrosion*; Macmillan: New York, 1992.
(76) Renock, D.; Mueller, M.; Yuan, K.; Ewing, R. C.; Becker, U. The energetics and kinetics of uranyl reduction on pyrite, hematite, and

magnetite surfaces: A powder microelectrode study. *Geochim. Cosmochim. Acta* **2013**, *118*, 56−71.
(77) Sarathy, V.; Tratnyek, P. G.; Nurmi, J. T.; Baer, D. R.; Amonette, J. E.; Chun, C.; Penn, R. L.; Reardon, E. J. Aging of iron nanoparticles in aqueous solution: effects on structure and reactivity. *J. Phys. Chem. C* **2008**, *112*, 2286−2293.
(78) Gallagher, P. T.; Oates, W. A. Partial excess entropies of hydrogen in metals. *Trans. Metall. Soc. AIME* **1969**, *245*, 179−182.
(79) Harinipriya, S.; Sangaranarayanan, M. V. Hydrogen evolution reaction on electrodes: Influence of work function, dipolar adsorption, and desolvation energies. *J. Phys. Chem. B* **2002**, *106*, 8681−8688.
(80) Lee, H. M. The solubility of hydrogen in transition metals. *Metall. Trans. A* **1976**, *7*, 431−433.
(81) Kita, H. Periodic variation of exchange current density of hydrogen electrode reaction with atomic number and reaction mechanism. *J. Electrochem. Soc.* **1966**, *113*, 1095−1106 discussion 1107−1010..